Weak correlation of starch and volume in synchronized photosynthetic cells

M. Michael Rading,[1,*] Michael Sandmann,[2] Martin Steup,[3] Davide Chiarugi,[1] and Angelo Valleriani[1,†]
[1]*Department of Theory and Bio-Systems, Max Planck Institute of Colloids and Interfaces, 14476 Potsdam, Germany*
[2]*innoFSPEC, Institut für Chemie, Universität Potsdam, Physikalische Chemie, 14476 Potsdam, Germany*
[3]*Department of Molecular and Cellular Biology, College of Biological Science, University of Guelph, Guelph, Ontario, Canada N1G 2W1*
(Received 22 August 2014; published 28 January 2015)

In cultures of unicellular algae, features of single cells, such as cellular volume and starch content, are thought to be the result of carefully balanced growth and division processes. Single-cell analyses of synchronized photoautotrophic cultures of the unicellular alga *Chlamydomonas reinhardtii* reveal, however, that the cellular volume and starch content are only weakly correlated. Likewise, other cell parameters, e.g., the chlorophyll content per cell, are only weakly correlated with cell size. We derive the cell size distributions at the beginning of each synchronization cycle considering growth, timing of cell division and daughter cell release, and the uneven division of cell volume. Furthermore, we investigate the link between cell volume growth and starch accumulation. This work presents evidence that, under the experimental conditions of light-dark synchronized cultures, the weak correlation between both cell features is a result of a cumulative process rather than due to asymmetric partition of biomolecules during cell division. This cumulative process necessarily limits cellular similarities within a synchronized cell population.

DOI: 10.1103/PhysRevE.91.012711 PACS number(s): 87.17.Ee, 87.17.Aa, 87.10.Mn

I. INTRODUCTION

For technical reasons, most studies in the Ohmic area require the analysis of relatively large cell populations. Essentially, this approach implies that the average values obtained from population measurements closely reflect data from single cells. However, this assumption is safe only when the cells composing a given population are homogeneous with respect to their physiological state, to their developmental states, and to the content of the analytes to be assayed.

For obtaining homogeneous cell populations, experimentalists rely on various techniques. To maintain both constant efficiency of external conditions and unchanged cell density, continuous cultures are typically used in which the culture medium is continuously renewed [1]. Under these conditions, the average growth rate can be adjusted to a constant value, i.e., the so-called steady-state or bound growth. The number of cells per suspension volume can also be kept constant if the number of daughter cells released exactly matches the number of cells lost through the outflow of the culture vessel. Uniformity of the cellular developmental state is obtained by synchronization techniques. These approaches aim at establishing cell cultures that, temporarily or permanently, will reside in the same phase of the cell cycle. To achieve this goal, various methods exist [2–4].

Nevertheless, single-cell analyses are providing increasing evidence that a truly homogeneous cell suspension is more difficult to obtain than expected. Indeed, the single cells composing isogenic populations can be largely different from each other even when they are grown in the same environment [5]. The reasons for the heterogeneity at the cellular level have been investigated for several model systems, including prokaryotic and eukaryotic cells, indicating that stochasticity in gene expression and cell division can play a major role [5–7]. However, the impact of these sources of stochasticity on synchronized cell cultures is still not completely understood and must be carefully taken into consideration. We address this issue in this paper. In particular, we focus on the unicellular eukaryotic alga *Chlamydomonas reinhardtii*, which is one of the most studied plant model organisms.

When grown photoautotrophically, the vegetative cell cycle of *C. reinhardtii* depends on the photoperiod. During the light period, photosynthesis drives the growth of cell volume, the DNA replication, and the biosynthesis of all other cellular constituents. The transition to the dark phase instead marks the release of daughter cells. These features are typically used for continuous synchronization of photoautotrophic cells. Exposing a cell culture of unicellular algae, such as *Chlorella* or *Chlamydomonas*, to a relatively short alternating series of light-dark phases results into a population that, at the onset of the light-dark cycle, consists essentially of young and small daughter cells. Photosynthesis-driven growth continues during illumination, leading to cell division and finally to the release of the offspring [8,9]. Readers interested in a comprehensive overview of the development of synchronized algal cells can consult Ref. [10].

Single-cell analyses, however, provide a different view on the homogeneity of synchronized cell cultures. Indeed, as reported in [11], synchronized cells of *C. reinhardtii* exhibit a relatively broad distribution of both cell sizes v and the cellular starch content y as shown by the coefficients of variation of cellular starch density, which ranges between 0.51 and 0.63. For the details about this issue, we refer the reader to Appendix A. Moreover, throughout the entire cell cycle, v and y are only weakly correlated [11]. Indeed, the Spearman rank correlation coefficient between relative cellular starch content and cellular volume ranges from 0.08 to 0.30, thus confirming that there is no obvious correlation. This finding is surprising because, intuitively, larger cells are expected to contain more starch than smaller cells. Furthermore, one may ask whether this counterintuitive experimental finding holds also for other cellular constituents. Our results will show that the ingredients

*rading@uni-potsdam.de
†angelo.valleriani@mpikg.mpg.de

causing the weak correlation are not specific to starch, thus indicating that this phenomenon is likely to apply to other metabolites as well.

This weak correlation between volume and other cellular constituents plays a major role in determining the heterogeneity of synchronized cultures, together with other peculiarities of *C. reinhardtii*, such as its characteristic cell division process, which consists of a sequence of binary divisions. According to a widely accepted view, the size of the offspring formed by a single cell is determined by the size of the mother cell at the time of cell division [12,13] and the division time is short compared to other time scales (e.g., the duration of fission bursts), at least under the conditions considered in [11]. The cellular volume of any eukaryotic unicellular organism is thought to define the onset of cell division [14].

The interplay of all cellular features outlined above points towards a higher degree of heterogeneity in synchronized *C. reinhardtii* cells. In this paper we present a more realistic model of a synchronized cell population. The model embeds in a coherent framework the potential sources of variability outlined above. In the following we will build the model in subsequent steps. Starting from a very basic description of the cellular volume growth, we progressively include all the relevant sources of heterogeneity in our model.

II. THEORY AND MODEL

In a very general scenario the volume growth rate of each cell can be regarded as depending on its age τ and on its volume v [15]. In a synchronized culture, τ coincides with the observational time, counting from the onset of each synchronization period. Thus, the cell volume growth during the light period is deterministic and can be effectively described by the growth rate function

$$\frac{dv}{d\tau} = f(v). \tag{1}$$

In (1) we assume that the impact of an increasing cell density on the growth process can be ignored given that experiments are performed in sufficiently diluted cell cultures. The volume growth law of algal organisms such as *Chlamydomonas* can be modeled after weakly curved functions. Hence, we assume that the power law

$$f(v) = f_\alpha v^\alpha \tag{2}$$

holds. The curvature of this function is low if α is close to 1. Values $\alpha < 1$ imply the concave form of the growth rate function. Although (2) is well supported by empirical data collected under the growth conditions used in [11], an approximate growth law of this kind can be postulated by assuming that cells are approximately spherical and that cell growth is determined by the surface of the sphere, which gives $\alpha = 2/3$. In general, deviations from this growth law should be expected at very large cell volumes, which have been reported for these growth conditions.

The two parameters α and f_α are sufficient to determine the curvature and slope of $f(v)$ for the empirical data presented in this paper. The power law (2) is particularly suited for analyzing multiple-cell division as occurring in *C. reinhardtii* [15]. In various strains of *C. reinhardtii* values of α were found to be in the range $\alpha \in (0.85\text{–}0.95)$ (see also [16]). Presumably, values of α exceed $2/3$ as light absorbance by the cellular chlorophyll rather than the uptake of nutrients from the medium limits growth. After 12 h light, cells are darkened and this transfer arrests volume growth. Cell volume remains essentially constant during the entire dark period.

In synchronization experiments the transition from light to dark marks the time when daughter cells are released. However, this timing is not precise and does not take place at exactly one time point (see, e.g., [17]). At the single-cell level, the release of daughter cells (as well as the preceding cell division) apparently lacks synchrony. Rather it proceeds over several hours and is, to some extent, affected by stochasticity. As revealed by detailed single-cell analyses, this is also true for the preceding cell division. When cells are grown under conditions of high productivity multiple-cell division occur frequently. Stochastic elements will be introduced into the model later. Furthermore, two assumptions are made in the model presented here. First, the release of daughter cells immediately follows the last cell division. Second, both cell division and the release of daughter cells are affected by the same stochastic elements.

Figure 1 illustrates possible division times $\tau_1, \tau_2, \ldots, \tau_n$ that all are occurring shortly before the light-dark transition. The times T_{light} and T_{dark} indicate the boundaries of the two synchronization periods. In the following we suppose that division times τ_k obey a characteristic distribution density function $\Psi(\tau)$ with well-defined standard deviation σ_τ and average value $\overline{\tau}$. The ratio of both numbers defines the coefficient of variation $\mathcal{C}_\tau$, which indicates how strongly division times of individual cells are scattered around the average value.

It is also reasonable to assume that asymmetric division is a source of noise and consequently increases the cell-to-cell diversity in populations (see, e.g., [18]). In the case of binary-cell division the volume of two newly formed daughter

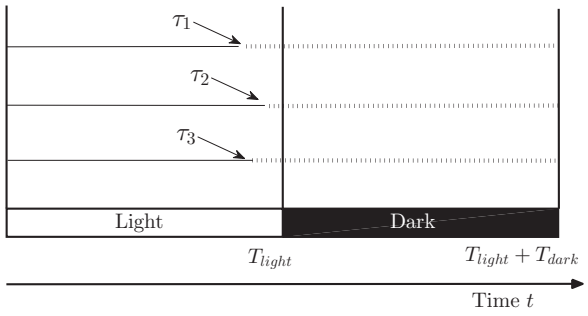

FIG. 1. Schematic representation of the timing of the cell division of *C. reinhardtii* embedded in the dark-light cycle. For the sake of readability, only two subsequent periods of the cycle are considered. The time τ_k represents the time instant of cell division. The figure illustrates the fate of three different cells. Note that τ_1, τ_2, and τ_3 are different, according to our assumption stating that cell division starts at a random time $\tau_k \leqslant T_{\text{light}}$. Consequently, a new cell cycle begins in the vicinity of the light-dark transition, following immediately the release of daughter cells. However, as reported in the text, the time intervals $T_{\text{light}} - \tau_k$ are negligible with respect to the duration of the light period.

cells (DCs) is $v_1 = \lambda v_{\rm div}$ and $v_2 = (1-\lambda)v_{\rm div}$, where λ is assumed to be a random variable with average $\overline{\lambda} = 0.5$ and coefficient of variation $\mathcal{C}_\lambda = \sigma_\lambda/\overline{\lambda}$.

Following [19], the growth process of individual cells is cast into a time-discrete model that describes the size distribution at the onset of the growth phase. In this context the index k numbers the light-dark cycles. We consider $f(v)$ to take the format displayed in Eq. (2). Moreover, any cell division requires photosynthesis-driven growth, therefore time points satisfy $\tau_k \leqslant T_{\rm light}$. After division, growth continues until cells have approached $T_{\rm light}$. However, an effect of synchronization is to push the beginning of the division time τ_k very close to the end of the light period. As a consequence, the time interval $T_{\rm light} - \tau_k$ becomes usually small in comparison to τ_k and thus this little growth of the daughter cells before the onset of the dark phase will be neglected here. Nevertheless, we will keep considering the effects of stochasticity of τ on the variation of the volume and starch content, as we will see. Hence, the balance of growth and division results in the time-discrete equation

$$v_{k+1} \approx \lambda_k \left[v_k^{1-\alpha} + f_\alpha (1-\alpha)\tau_k \right]^{1/(1-\alpha)}, \tag{3}$$

which relates the volume v_k that the mother cell had at birth with the volume v_{k+1} that the daughter cell has when released. Equation (3) relates the volumes of mother and daughter cells along a single line of the cell division tree. This implies that the statistical distribution of the cell ensemble in cycle k reflects the statistical properties along the time path derived from Eq. (3) over infinite generations $k = 1,2,\ldots,\infty$.

Size plays an important role in the control of the cell cycle [10]. For this reason we presume size-dependent growth of starch content y. The accumulation rate of starch, for instance, can be directly linked to the cell volume. Hence, the time course of $v(\tau)$ determines the dynamics of $y(\tau)$. We assume therefore that there is a function $h[v(\tau)]$ that captures the synthesis rate of starch at each time point τ during the light period. For the moment we leave the function h unspecified, but we will discuss its specific form for starch later. This assumption leads to the growth equation

$$\frac{dy}{d\tau} = h[v(\tau)]. \tag{4}$$

Integration of Eq. (4) yields

$$y(\tau) = y(0) + H[v(\tau)] - H[v(0)], \tag{5}$$

where $H(x)$ is defined as the antiderivative

$$H[v(\tau)] = \int^{v(\tau)} dx \frac{h(x)}{f(x)}. \tag{6}$$

At the time of division cell content $y(\tau = \tau_{\rm div})$ is distributed among daughter cells. According to Eq. (3), the mother cell has reached the size $v(\tau_{\rm div}) = v_{k+1}/\lambda_k$ at this point. Notice that both $f(v)$ and $h(v)$ are strictly positive functions, so both variables v and y are monotonically increasing with age τ.

After combining Eq. (4) with degradation and asymmetric partitioning, we obtain the time-discrete process describing y:

$$y_{k+1} = \gamma_k m_k \left(y_k + H\left[\frac{v_{k+1}}{\lambda_k} \right] - H[v_k] \right), \tag{7}$$

where we assume that partitioning of starch content y is governed by the random variable $\gamma_k \in (0,1)$, which is not necessarily identical to λ_k used in Eq. (3) to describe the partitioning of the cell volume. The parameter $m_k \leqslant 1$ in (7) instead takes the possible degradation process into account. The random multiplier m_k, which describes the decrease of y subsequent to cell division, encodes our assumption that degradation is a stochastic process. In particular for starch this term is biologically meaningful since starch is metabolized by the cell during the dark period as a source of energy. As we will discuss later, the parameter m_k is not a determinant of the weak correlation between the cell parameters v and y. Equations (3) and (7) constitute the basic model for analyzing the distributions of y and v, as well as the correlation between these two cell parameters.

III. CELL SIZE DISTRIBUTION

We denote the probability density of cell volume at the onset of each synchronization by $\Phi(v)$. The shape of $\Phi(v)$ results from growth and division of individual cells (see [18]). One method of analyzing the distributions analytically makes use of renewal equations, which describe the population balance of dividing cells and newly generated daughter cells (see, e.g., [20]). We use the discrete process in Eq. (3) and derive an approximate expression for the size distribution $\Phi(v)$.

A. Asymmetric binary division

Equation (3) is a nonlinear autoregressive equation in which τ_k and λ_k are noisy parameters. Both affect the formation of the size distribution at the beginning growth phase. We will use the notation Δ^x to describe the relative deviation Δx of parameter x from its average $\overline{x}$, that is,

$$\Delta_k^x \equiv \frac{x_k - \overline{x}}{\overline{x}}. \tag{8}$$

Furthermore, we assume that fluctuations around the steady state are small, which implies $\mathcal{C}_\tau \ll 1$ and $\mathcal{C}_\lambda \ll 1$. This can be experimentally shown for deviations of the average division time of cells of *C. reinhardtii* (see, e.g., [21]), where the coefficient of variation takes values $\mathcal{C}_\tau \leqslant 0.1$.

From Eq. (3) it is possible to derive an equation for Δ_k^v and thus obtain a derivation of the coefficient of variation, if one notices that

$$\mathcal{C}_x^2 = \left\langle \left(\Delta_k^x\right)^2 \right\rangle_k. \tag{9}$$

In the case that noise terms Δx_k are uncorrelated, the following relation for the variation coefficients holds (see Appendix B for details of the derivation):

$$\mathcal{C}_v^2(\alpha) \approx \frac{1}{1-2^{2(\alpha-1)}} \left(\mathcal{C}_\lambda^2 + \frac{1-2^{\alpha-1}}{1-\alpha} \mathcal{C}_\tau^2 \right). \tag{10}$$

Equation (10) shows to what extent $\mathcal{C}_\tau$, $\mathcal{C}_\lambda$, and the parameter α influence the heterogeneity of cell sizes. A comparison of this result with computer simulations is shown in Fig. 2.

If the growth rate function is weakly sloped the parameter $1-\alpha$ becomes very small and amplifies the variation coefficient $\mathcal{C}_v$. Furthermore, it can be shown (see Appendix B) that the underlying process (3) generates naturally the log-normal

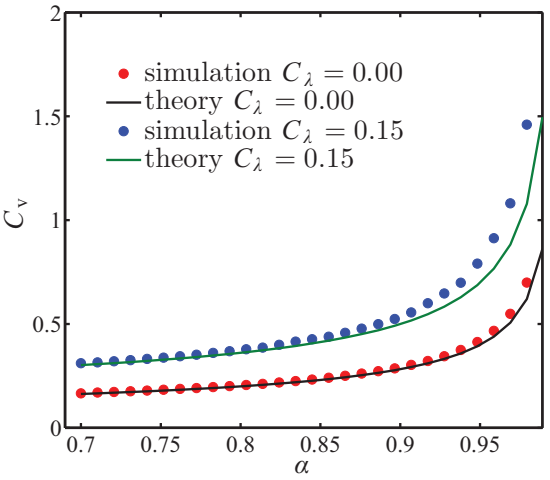

FIG. 2. (Color online) Comparison between the theoretical result of Eq. (10) and computer simulations of the binary division process with a fixed value of $f_\alpha = 0.3\ \mu\mathrm{m}^{1-\alpha}\ \mathrm{h}^{-1}$ and different magnitudes of the parameter $\mathcal{C}_\lambda$ to describe asymmetric cell division. The lower curve corresponds to $\mathcal{C}_\lambda = 0$ and the higher curve to $\mathcal{C}_\lambda = 0.15$. Cell age at division obeys the Weibull distribution density function $\mathrm{We}(\tau_c,a,b)$ with the parameters $\tau_c = 2$ h, $a = 2$ h, and $b = 3.4$. Under this assumption, a coefficient of variation with the value $\mathcal{C}_\tau \approx 0.1$ is obtained.

distribution of cell volumes that is so universally observed in single-cell populations of many different organisms.

B. Multiple-cell division

As mentioned earlier, *C. reinhardtii* cells do not necessarily form a progeny of two equally sized cells but often divide into 2^n daughter cells. Therefore, we introduce a probability $\pi_n(\tau|v_{(i)})$ that tells us how likely it is that a mother cell divides into exactly 2^n daughter cells given its age τ at division and its initial size $v_{(i)}$. It is assumed that on average the fold change of cell volume $v(\tau)/v_{(i)}$ during the growth phase determines the number of progeny (compare, e.g., [22]). This implies the dependence of the probability π_n on the size ratio $v/v_{(i)}$ that manifests in the functional form $\pi_n(v/v_{(i)})$.

Apart from that, Eq. (2) implies the unique relation between age τ and the cell volumes v and $v_{(i)}$. We can simplify the treatment further if we recognize, based on the experimental data, that α is very close to unity and thus that cell volume growth is nearly exponential. As a consequence of the exponential growth of the volume, the ratio $v/v_{(i)}$ turns out to depend only on the time of division. This means that π_k becomes independent of v and $v_{(i)}$ and thus dependent only on the timing of cell division. If division times are concentrated around the average value $\overline{\tau}$, we can approximate the random division times τ_k by the average $\overline{\tau}$. Here the time $\overline{\tau}$ roughly coincides with the length of the light period T_{light}. Hence, since T_{light} is fixed by the experimental conditions, the probabilities $\pi_n = \pi_n(\overline{\tau})$ are considered constant throughout one set of experiments under fixed light-dark conditions.

The net productivity can be defined as the average relative fold change of the cell number at the end of one cell cycle. Using π_n, the relative fold change in population size is determined by the weighted average $\overline{N} = \sum_{n=1}^{\infty} 2^n \pi_n$. Since division occurs with constant probability π_n, the parameter λ_k introduced in Eq. (3) is a random number whose probability distribution is

$$P(\lambda_k = 2^{-n}) = \frac{2^n}{\overline{N}}\pi_n. \tag{11}$$

Obviously, π_n is weighted by the relative number of progeny resulting in 2^n daughter cells, which is $2^n/\overline{N}$.

Consequently, in the light of Eq. (3) multiple division appears as a particular form of binary asymmetric cell division. This parallel is clearly restricted to the use that we intend to make of Eq. (3). Nevertheless, it has far reaching consequences, because we can now use the simpler results obtained earlier for the binary asymmetric cell division and derive the statistics of the cell volume by simply adjusting the parameter λ_k.

Indeed, the average value of λ_k is now $\overline{\lambda} = \overline{N}^{-1}$, while the coefficient of variation $\mathcal{C}_\lambda$ is determined by $\sigma^2 = \sum_{n=0}^{\infty} \overline{N}^{-1} 2^n \pi_n 2^{-2n} - \overline{N}^{-2}$. Hence, the explicit expression for $\mathcal{C}_\lambda$ reads

$$\mathcal{C}_\lambda^2 = \overline{N} \sum_{n=0}^{\infty} \frac{\pi_n}{2^n} - 1. \tag{12}$$

For clarification we use data of *C. reinhardtii* CC1690 that divide on average into $\overline{N} = 14$–15 daughter cells under the conditions described in [11]. We estimate the probabilities π_n with $\pi_3 = 0.2$ and $\pi_4 = 0.8$, by which the mother cell produces 8 DCs or 16 daughter cells, respectively. After inserting these numbers in Eq. (12), we obtain $\mathcal{C}_\lambda \approx 0.3$, which serves as an orientation for the upcoming analysis.

If we make the heuristic argument that mother cells produce $\overline{N}$ instead of two daughter cells in one cycle we can replace $2^{1-\alpha}$ by $\overline{N}^{1-\alpha}$ in Eq. (10) (compare with Appendix A). By exploiting the analogy with the asymmetric binary division, directly from Eq. (10) we obtain the coefficient of variation

$$\mathcal{C}_v^2 = \frac{1}{1-\overline{N}^{2(\alpha-1)}}\left[\mathcal{C}_\lambda^2 + \left(\frac{1-\overline{N}^{\alpha-1}}{1-\alpha}\right)^2 \mathcal{C}_\tau^2\right], \tag{13}$$

where we see that large numbers of progeny, i.e., large $\overline{N}$, increase the relative impact of $\mathcal{C}_\tau$ in comparison to $\mathcal{C}_\lambda$. If $\alpha \lesssim 1$ holds, we will make use of the approximation $1-\overline{N}^{\alpha-1}/(1-\alpha) \approx \ln \overline{N}$. As a side result, by exploiting the similarity to the asymmetric binary division, we obtain the explicit expression for the cell volume probability density $\Phi(v)$ under the multiple-cell division scenario, as shown in Eq. (B12). A comparison with the empirical data, shown in Fig. 3, provides an excellent fit.

IV. CORRELATION BETWEEN CELL PARAMETERS

We aim to elaborate the mechanisms that cause the weak correlation between the cell parameters. These are the asymmetric division of cell content and the accumulation process and its dependence on the cell volume. We will further incorporate degradation of starch during the dark period. As will be shown below, degradation processes are not major

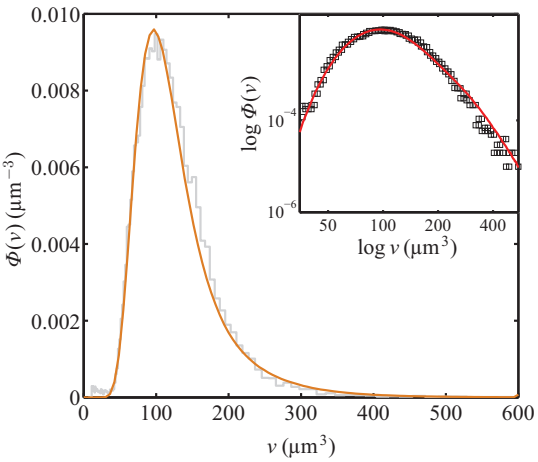

FIG. 3. (Color online) Size distribution of synchronized cells of *C. reinhardtii* (strain CC 1960) at the onset of the light-dark cycle in comparison to theoretical results. The parameters are $\alpha = 0.85$, $\mathcal{C}_\tau = 0.1$, and $\mathcal{C}_\lambda = 0.25$ with $\pi_3 = 0.18$, $\pi_4 = 0.82$, and $\overline{N} = 14.6$ (the continuous line corresponds to a solution based on the numerical integration of the theory and the histogram corresponds to data from [11]). The inset depicts the double logarithmic ($\log_{10}$ scale) representation of the same data. The distribution density function is obtained by numerically solving Eq. (3) [23,24] under the assumption of Weibull-distributed times of daughter cell release with the parameters $\tau \sim \mathrm{We}(\tau_c,a,b)$, with $a = 4$ h, $b = 3$, and $\tau_c = 9.8$. The fit of parameters gives good agreement for $\alpha = 0.86$ and $f_\alpha = 0.72$. The intergenerational correlation of cell sizes is approximately $E[\Delta_{k+1}^v \Delta_k^v] = \overline{N}^{\alpha-1} \approx 0.7$. Details of the experimental procedure can be found in Ref. [11] and are summarized in Appendix A.

determinants for the weak correlation between cell volume and starch content.

Equation (3) describes a process that generates the size distribution of multiply dividing *C. reinhardtii* cells. We argue that size is fundamental for the understanding of the starch distribution in cells. This is due to the fact that starch accumulation can be unambiguously linked to the cell cycle, which in turn relies on volume growth. As a consequence, Eq. (7) determines the distribution of y at the onset of each synchronization cycle.

To give an example, we consider a situation in which the synthesis rate of y is proportional to the growth rate $f(v)$. Thus, we have $h(v) = cf(v)$ with an unspecified constant c. For the sake of simplicity, we assume symmetric division into exactly $N = 2^n$ daughter cells. This assumption implies that $\mathcal{C}_\gamma = \mathcal{C}_\lambda = 0$. If $N \gg 1$ holds, as it is the case for *C. reinhardtii*, we can justify the elimination of y_k and $H[v_k]$ from Eq. (7). As a result, the problem is reduced to a dynamical equation of the form

$$y_{k+1} \simeq c v_{k+1}. \tag{14}$$

Equation (14) implicates that the size distribution $\Phi(v)$ simultaneously determines the statistical distribution of the starch content per cell. In this case we obtain perfect correlation between both cell parameters that give rise to a high product-moment correlation [$\mathrm{Corr}(v,y) = 1$]. However, in reality one observes a quite distinct behavior. The broad distribution of starch content and the weak correlation with the cell volume in *C. reinhardtii* cells demonstrates this exemplarily. We must therefore identify mechanisms that lead to the characteristic distribution and correlation function of both cell parameters.

The discussion below will focus on two mechanisms that both contribute to the observed cell-to-cell diversity: the asymmetric partitioning of cell content and the functional form of the starch accumulation process.

A. Asymmetric distribution of cell content

The characteristic distribution of the amount of starch per cell emerges partially as a result of asymmetric partitioning of cell content during the division process. Obviously, the asymmetric distribution of y increases the heterogeneity of the starch distribution. We already know from experiments (see, e.g., [13,25]) that cell division into 2^n daughter cells can be viewed as the fast iteration of n bisections. In accord, with experimental observations, we assume that daughter cells have equal size after each bisection, while the partitioning of the starch content is subject to asymmetries.

Since starch is stored in the chloroplast, it is bound to the physical structure of the organelle. We can therefore argue that asymmetries arise from the uneven division of organelles or the patchy storage of starch at different locations of the chloroplast, which both lead to an irregular endowment of cells with starch content.

We describe asymmetric division with the help of n independent and identically distributed random numbers $\gamma^{(1)},\gamma^{(2)},\ldots,\gamma^{(3)}$, where the superscript index (l) numbers the sequence of bisections. The numbers $\gamma^{(l)}$ capture the stochastic distribution of starch content during the division process. The average of these random numbers is each $\overline{\gamma^{(l)}} = 1$, while the coefficient of variation satisfies $\mathcal{C}^l = \mathcal{C} = \mathrm{const}$ at each instance. Since the partitioning of y results from n bisections, the product of all the partitions determine γ_k in Eq. (7), i.e., we have after n bisections

$$\gamma_k = \frac{1}{2}\gamma_k^{(1)}\frac{1}{2}\gamma_k^{(2)}\cdots\frac{1}{2}\gamma_k^{(n)} = \frac{1}{2^n}\prod_{l=1}^{n}\gamma_k^{(l)}. \tag{15}$$

Equation (15) implies that γ_k and the variation Δ_k^γ depend on the total number of bisections n, that is, $n \sim -\ln\lambda_k$. The calculations of the coefficient of variation $\mathcal{C}_\gamma$ are performed in Appendix B and lead to an approximate expression

$$\mathcal{C}_\gamma^2 = \mathcal{C}_\lambda^2 + \sum_{n=1}^{\infty} n\pi_n \frac{\overline{N}^2}{2^{2n}}\mathcal{C}^2, \tag{16}$$

which takes multiple division and asymmetric partitioning of cell content into account. Here $\mathcal{C}_\lambda$ is calculated according to Eq. (12) and allows for different forms of multiple-cell division; $\mathcal{C}_\gamma$ measures the variation of the amount of starch in an arbitrarily chosen sample of synchronized cells. If mother cells divide irregularly and into different numbers of daughter cells, $\mathcal{C}_\lambda$ will outweigh the effect of the asymmetric distribution of starch.

Since experiments are not indicative of a very strong asymmetric distribution of starch content, we estimate $\mathcal{C} \leqslant 0.1$ to be a realistic range of values for $\mathcal{C}$. Note, however, that this estimate gives $2\mathcal{C} = 0.2$ for $n = 4$ consecutive bisections and the symmetric division into $2^n = 16$ equally sized daughter

cells [see Eq. (16)]. The value $\mathcal{C} = 0.1$ clearly overestimates the impact of asymmetric distribution of starch and we therefore conclude that $\mathcal{C}$ is likely well below this value.

We illustrate a realistic case by choosing the parameters $\overline{N} = 15$, $\pi_3 = 0.2$, $\pi_4 = 0.8$, $\mathcal{C}_\lambda \approx 0.3$, and $\mathcal{C}_v = 0.5$ for a *C. reinhardtii* CC1690 culture. The value of $\mathcal{C}_\gamma$ is determined through Eq. (16), which yields $\mathcal{C}_\gamma \approx 0.34$ for the given set of parameters. Consequently, $\mathcal{C}_\gamma$ keeps relatively close to the value of $\mathcal{C}_\lambda$. In summary, this means that the coefficient of variation $\mathcal{C}_\lambda$ related to the division in a random number of daughter cells almost completely determines the value of the coefficient of variation $\mathcal{C}_\gamma$. The latter instead is related to the asymmetric partitioning of starch content to the daughter cells. Hence, this indicates that the asymmetric partitioning of starch content is determined more by the stochasticity in the number of daughter cells than by the random process that governs the redistribution of cell content. If, however, we had a dominant form of division, we would have observed a pattern of cell division that produced 2^n descendants at each iteration of the synchronization cycle. In this case, the heterogeneity of the distribution of starch can originate only from the second term on the right-hand side of Eq. (16) and thus from the asymmetric partitioning.

B. Starch accumulation

Let v_{k+1} be the size in the $(k+1)$th synchronization cycle. Preliminary considerations led to Eq. (7) and showed that v_{k+1} and the initial size v_k of the mother cell determine the starch content y_{k+1} at the $(k+1)$th cycle. Hence, y_{k+1} becomes almost proportional to the difference $H[N v_{k+1}] - H[v_k]$. For simplicity, we will further consider an approximation of Eq. (7) by eliminating the contribution of the term $\overline{N}^{-1} y_k$. This is possible since $\overline{N}$ becomes large in the considered case. Given a fixed size v_{k+1}, it is the size v_k of the progenitor cell that determines the starch content through the relation $y_{k+1} \sim H[N v_{k+1}] - H[v_k]$.

Equation (3) leads to the approximate expectation value $E[v_{k+1}|v_k] \approx v_k$ for parameter choices $\alpha \lesssim 1$. If we reverse the process and use a simple symmetry argument, we can state the conditional expectation value $E[v_k|v_{k+1}] \approx v_{k+1}$ for sizes v_k of the preceding cycle in order to obtain v_{k+1} (compare, e.g., Appendix B).

Similarly, we introduce a coefficient of variation $\widetilde{\mathcal{C}}_v$ that quantifies the region in the vicinity of $E[v_k|v_{k+1}]$ from where progenitor cells most likely originate. This simply means that the values of v_k are spread around their expectation value, while the variation $\widetilde{\Delta}_k^v$ around this expectation value is conditional on the size in the $(k+1)$th cycle. For $\alpha \approx 1$ and relatively small variation of the division times $\mathcal{C}_\tau$, we use the estimate $\widetilde{\Delta}_k^v \approx \Delta_k^v$. In this situation the coefficient of variation satisfies $\widetilde{\mathcal{C}}_v \approx \mathcal{C}_v$. However, it should be noted that parameters $\alpha < 1$ and large values of $\mathcal{C}_\lambda$ and $\mathcal{C}_\tau$ considerably complicate the calculation of $\widetilde{\mathcal{C}}_v$ but do not result in different qualitative results.

We can now discuss the impact of the deviations $\widetilde{\Delta}_k^v$ on the fluctuation of the parameter y_{k+1}. To that end we assume v_{k+1} to take a fixed value in the $(k+1)$th cycle. Hence, the magnitude of the fluctuations of y_{k+1} around the average $\overline{y}_{k+1}$ measures how heterogeneously starch is distributed in cells with the fixed size v_{k+1}. Due to this mechanism, the correlation between size and starch content decreases as the outcome of the fluctuations of cell sizes in two consecutive cycles.

To show this we evaluate the first-order derivation of $H[v_k]$ at the size $E[v_k|v_{k+1}] \approx v_{k+1}$ and calculate the variation Δ^y of y. The result is a relation between the fluctuations of the starch content Δ_{k+1}^y and the fluctuations of cell sizes, i.e.,

$$\Delta_{k+1}^y(v_{k+1}) \approx \frac{H'(v_{k+1})v_{k+1}}{H(\overline{N}v_{k+1}) - H(v_{k+1})}\Delta_k^v. \tag{17}$$

Equation (17) demonstrates that fluctuations of y_{k+1} around the average $\overline{y}(v_{k+1})$ depend on the value of v_{k+1}. For this reason the factor in front of Δ^v measures the strength of fluctuations as a function of cell size v.

Equation (17) allows us to compare different types of accumulation processes. In what follows we assume that $h(v)$ is a monotonically increasing function of size v. In the simplest case $h(v)$ is proportional to the growth rate $f(v)$, which leads to the expression $H[v] = cv$ and the unspecified constant c. If we plug $h(v)$ into Eq. (17) and if we further assume $\overline{N} \gg 1$, we obtain the relation $\Delta_{k+1}^y \simeq \overline{N}^{-1}\widetilde{\Delta}_k^v$. However, this means that $\mathcal{C}_y$ will be small in comparison to $\mathcal{C}_v$ if $\overline{N}$ becomes large. By this means both parameters, size and starch content, are tightly correlated.

By having a closer look at Eq. (17) we see that it is the ratio of $H'[v]v$ and $H[\overline{N}v] - H[v]$ that determines how strongly y fluctuates around its mean value. If the absolute value $|H[v]|$ is rapidly decreasing in the vicinity of $\overline{v}$, the contribution of $|H[\overline{N}v]|$ becomes negligible for very productive forms of cell division. We want to describe this behavior more clearly and consider the function

$$h(v) = \frac{A}{\{1 + [\eta(v/\overline{v})]^B\}^2}\left(\frac{v}{\overline{v}}\right)^B, \tag{18}$$

which represents a family of functions that, when embedded in Eq. (4), correctly describes the experimental results reported in [11] and summarized in Fig. 1 therein. In particular, Eq. (18) takes into account the slowing down of the rate of starch production when cells become much larger than $\overline{v}$. A comparison of Eq. (18) with the empirical data reported in [11] shows that Eq. (18) is indeed a good model for describing the accumulation of starch during the light period. A reasonable choice of parameters for fitting the data mentioned above is $\eta \approx 0.5$–1.0 and $B \approx 2$. An analytically tractable case can be obtained if we integrate Eq. (18) under the assumption $f(v) \approx f_1 v$ and $B = 2$. With this choice of parameters Eq. (18) still results in a good fit for the experimental data related to cell growth and starch accumulation in

$$H(v) = -\frac{A}{1 + \eta^2(v^2/\overline{v}^2)}, \tag{19}$$

with the unspecified constant A. The model represented in Fig. 4 is based on Eq. (19) under the assumption of cell division into strictly $\overline{N} = 2^4 = 16$ daughter cells. It demonstrates how Δ_{k+1}^y is affected by the variation of sizes of the progenitor cell, i.e., $\widetilde{\Delta}_k^v$. According to Eq. (17), the magnitude of the

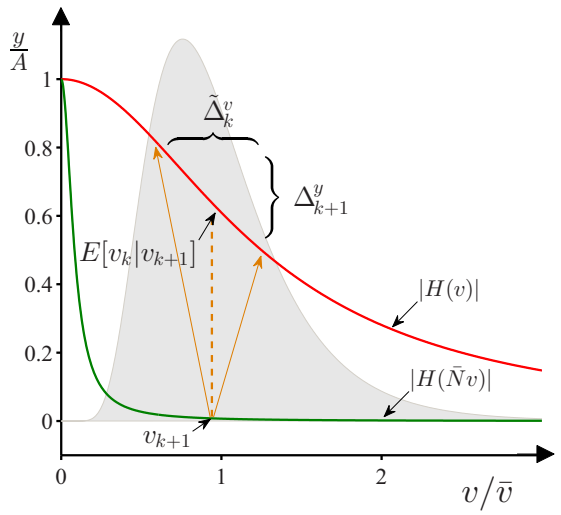

FIG. 4. (Color online) The behavior of y_{k+1} can be related to fluctuations of v_{k+1} in each cycle. The difference of the accumulation function $H(\overline{N}v) - H(v)$ on average determines the dependence of the parameter y on size v. Cell sizes are distributed around the average $\overline{v}$ and obey a log-normal distribution (gray area). The steep decrease of $|H(v)|$ compared to $|H(\overline{N}v)|$ for typical cell sizes $v \approx \overline{v}$ manifests in the sensitive response of $\Delta^y(v_{k+1})_{k+1}$ to deviations $\tilde{\Delta}_k^v$ in each cycle.

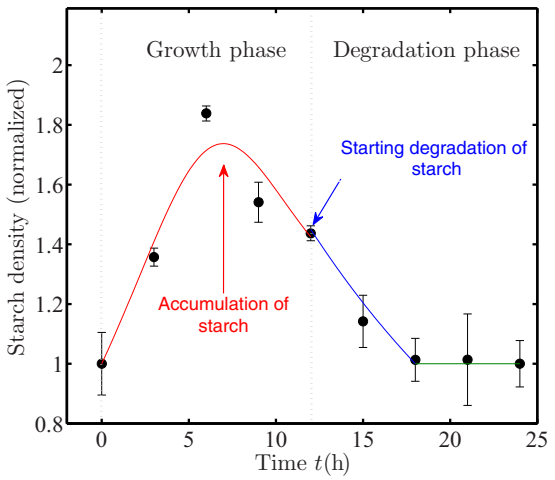

FIG. 5. (Color online) Dynamics of the average starch concentration in *C. reinhardtii* cells (normalized to the initial concentration $\overline{\varrho}$). Shown are periods of cell growth (light period, from time 0 to time 12 h) and degradation (initial 6 h of the dark period). The line across the data in the light period shows the fit function for $\rho(t)$ with the parameter $B = 1.93$.

fluctuations of y is given through

$$\mathcal{C}_y(v) \approx \frac{2\eta^2 v^2}{\overline{v}^2 + \eta^2 v^2}\widetilde{\mathcal{C}}_v. \tag{20}$$

Equation (20) establishes a relation between $\mathcal{C}_y$ on the one hand and v and $\mathcal{C}_v$ on the other. Since v_{k+1} is typically located in the vicinity of the average cell size $\overline{v}$, we can estimate the representative value for the coefficient of variation, which takes the form

$$\mathcal{C}_y(\overline{v}) \approx \frac{2\eta^2}{1+\eta^2}\mathcal{C}_v. \tag{21}$$

Here $\mathcal{C}_y$ exhibits a magnitude similar to that of $\mathcal{C}_v$ for the parameter region $\eta \approx 1$ and as a result the starch content y shows strong fluctuations around its mean value $\overline{y}(v)$. The discussed mechanism evidently mitigates the correlation between y and v and as the example shows is mainly encoded in the specific form of the function $h(v)$.

V. EXAMPLE

In [11] the authors show that the product moment correlation coefficient $\mathrm{Corr}(\varrho, v)$ between cell size and starch density in the alga *C. reinhardtii* CC1690 is strictly negative. Similarly, the rank correlation according to Spearman takes values in the range $\mathrm{Corr}_S(\varrho, v) = -0.50$ to -0.60. At the same time the correlation coefficient for starch and size takes the value $\mathrm{Corr}_S(v, y) \approx 0.2$. In order to explain these experimental results, we study the discrete equations (3) and (7) that determine the discrete-time starch concentration $\varrho_k = y_k/v_k$ in each cycle.

The synthesis rate of y is modeled after the concave function (18). By choosing $\eta = 0.5$ and $B = 1.93$ we obtain a decent description of starch accumulation during the whole light period. The time course of the starch density per cell reads $\varrho(t) \approx \overline{y}(t)/\overline{v}(t)$ and is shown in Fig. 5.

The experiments show that starch degrades when cells are darkened, leading to a decrease of starch content per cell. Degradation of starch contributes to (7) in the form of the random variable m_k, whose average is $\overline{m}^{-1} \approx 1.5$. It can be further assumed that m_k is conjecturally dependent on v and y. Appendix B contains a brief discussion of how the cell size can affect the degradation of starch and how size-dependent degradation contributes to the value of the product moment correlation coefficient. We note here that under plausible assumptions about the starch degradation mechanism, the functional form of $h(v)$ keeps the principle determinant for the strong fluctuations of size and starch content.

For the purpose of calibrating the theoretical model, we use the parameters $\alpha = 0.86$, $\overline{N} = 14.6$, $\mathcal{C}_\lambda = 0.3$, and $\mathcal{C}_\tau = 0.1$ from fitting the size distribution $\Phi(v)$ in Fig. 3. The cell size is then calculated on the basis of Eq. (3). We also incorporate the heterogeneous partitioning of starch content by assuming $\mathcal{C} \leqslant 0.1$. On average the starch density increases by the factor 1.5 during the light period (see Fig. 5) and decreases uniformly afterward. We do not consider a particular size-dependent form of the degradation process since it does not fundamentally change the theoretical results.

The example shows that the theoretical values of the product moment correlation $\mathrm{Corr}(v, y)$ and the rank correlation $\mathrm{Corr}_S(v, y)$ are consistent with experiments. We can now assess to what extent asymmetric division and the functional form of the accumulation rate $h(v)$ contribute to the joint distribution of both cell parameters. While moderate asymmetries ($\mathcal{C} \leqslant 0.1$) during the division process can partially explain the observed heterogeneity of the starch distribution, the form of the accumulation process $h(v)$ is the principle mechanism that leads to the strong fluctuation of both cell parameters, a weak correlation and a broad joint distribution of cell volume and starch content.

VI. CONCLUSION

In this paper we reported on a model that explains the origin of the multivariate statistics of cell parameters. We provided a mechanism that explains the cause of the log-normal-shaped size distribution of multiply dividing *C. reinhardtii* cells in a widely used synchronization setup. Nearly exponential growth and variations with respect to the timing of cell division and the growth process contribute to the considerable heterogeneity of cell populations. It was demonstrated that multiple-cell division can be regarded as a form of asymmetric division. The resulting distribution of cell sizes and their characteristic moments at the onset of each cell cycle are comparable for binary and multiple division. The theoretically obtained distribution density functions compare well with empirical data.

On the basis of the presumed cell cycle control by size, we elucidated the accumulation of starch per cell. The correlation analysis reveals that a mutual identification of this cell parameter with the help of cell volume is restricted by the form of the accumulation process. This has far reaching consequences. Under certain conditions it is possible to predict the value y by measuring a more accessible quantity, such as the cell volume. However, we can demonstrate on the basis of starch accumulation that for realistic forms of the size-controlled accumulation process starch content and cell volume are weakly correlated in each cycle. The heterogeneity manifests in a considerable variance of the starch content y for any given cell volume v. The potential asymmetric distribution of starch content additionally increases the described effect.

ACKNOWLEDGMENTS

We acknowledge financial support from the German Federal Ministry of Education and Research within the program Unternehmen Region (Grant No. 03Z2AN12) and GoFORSYS (Grant No. 0313924). A.V. thanks Katja Schulze for help with the manuscript.

APPENDIX A: SUMMARY OF EXPERIMENTAL SETUP AND RESULTS

Materials and methods

Vegetative cells of strain CC1690 from *Chlamydomonas reinhardtii* were obtained from the Chlamydomonas Resource Center, University of Minnesota, St. Paul, Minnesota (USA). Preculture and synchronization of the cells using photoautotrophic conditions were performed as described in [11]. Under standard conditions, synchronized cells were grown in a synthetic medium containing ammonium as nitrogen source, high light intensities (900 to 550 μmol photons $m^{-2}\,s^{-1}$ at the beginning and the end of the light period, respectively, as measured inside of the suspension) and 34 °C [11]. Cell volume was determined using a Beckman Coulter Counter MULTISIZER 3 (Beckman Coulter, Krefeld, Germany) as previously described [11]. Starch content was determined enzymatically using a photometric assay that is based on the conversion of starch-derived glucose to glucose 6-phosphate as mediated by hexokinase and glucose 6-phosphate dehydrogenase. Prior to the photometric assay, cells were broken by sonification in 80 vol% ethanol. Starch was solubilized by KOH and converted to glucose by amyloglucosidase treatment (Starch Assay Kit, R-Biopharm, Darmstadt, Germany). Tables I and II provide a summary of the key results used in this paper. For further details, see [11].

TABLE I. Summary of the Spearman correlation coefficient ρ computed in [11] between the relative starch content and the cellular volume, measured during the first 6 h of the light period in a synchronized cell culture of *C. reinhardtii* .

Time (h)	ρ starch vs volume
0	0.30
2	0.12
4	0.08
6	0.13

APPENDIX B: SIZE DISTRIBUTION AND MOMENTS

If perfectly timed, division always occurs at the average time point $\overline{\tau}$. Strictly binary division exhibits the average $\overline{\lambda} = \frac{1}{2}$. In order to determine the average cell volume $\overline{v}$ we expand the right-hand side of Eq. (3) in powers of Δ_k^τ, Δ_k^λ, and Δ_k^v and average over the contributing noise terms on both sides of the equation.

Equation (3) can be linearized in order to analyze the response of the system to noise. To this end we introduce the logarithm of cell size $u_k = \ln v/\overline{v}$, which is a good approximation if $1-\alpha$ becomes small. Taking the logarithm of v on both sides of Eq. (3) and expanding the expression around $\overline{v}$, we obtain

$$u_{k+1} = \overline{\lambda}^{1-\alpha} u_k + \Delta_k^\lambda + \frac{1-\overline{\lambda}^{1-\alpha}}{1-\alpha}\Delta_k^\tau. \tag{B1}$$

This linear autoregressive process is convergent since $\gamma = \overline{\lambda}^{1-\alpha} < 1$ holds for every choice of $\alpha < 1$. If noise terms Δ^x are small, we can approximate u_k by

$$u_k = \ln\frac{v_k}{\overline{v}} \approx \frac{\Delta v_k}{\overline{v}}. \tag{B2}$$

We next Taylor expand the right-hand side of Eq. (3) in orders of

$$\Delta_k^x = \frac{\Delta x_k}{\overline{x}}, \tag{B3}$$

where $\Delta x_k = x_k - \overline{x}$ denotes the deviation from the average $\overline{x}$. The result of the Taylor expansion of

$$\overline{v}\left(1+\Delta_{k+1}^v\right) = \overline{\lambda}\left(1+\Delta_k^\lambda\right)\left[\overline{v}^{1-\alpha}\left(1+\Delta_k^v\right)^{1-\alpha} + \cdots + f_\alpha(1-\alpha)\overline{\tau}\left(1+\Delta_k^\tau\right)\right]^{1/(1-\alpha)} \tag{B4}$$

TABLE II. Summary of the mean values and width 2σ of the cellular starch density distribution derived after the log-normal fit, computed in [11]. The errors refer to the 95% confidence intervals.

Time (h)	Mean starch density	2σ
0	2.34 ± 0.08	2.98 ± 0.2
2	4.22 ± 0.32	4.31 ± 0.7
4	10.23 ± 0.67	10.44 ± 1.5
6	15.92 ± 0.82	19.72 ± 2.08

up to second order reads

$$\overline{v}\left(1+\Delta_{k+1}^{v}\right)=\overline{\lambda}\left(1+\Delta_{k}^{\lambda}\right)[\overline{v}^{1-\alpha}+f_{\alpha}(1-\alpha)\overline{\tau}]^{1/(1-\alpha)} \times\left[1+a_{1}(\overline{v})\Delta_{k}^{v}+b_{1}(\overline{v})\Delta_{k}^{\tau}+c_{1}(\overline{v})\Delta_{k}^{\tau}\Delta_{k}^{v} +\cdots+a_{2}(\overline{v})\left(\Delta_{k}^{v}\right)^{2}+b_{2}(\overline{v})\left(\Delta_{k}^{\tau}\right)^{2}+\cdots\right]. \tag{B5}$$

In a first step we average this expression, where we assume $E(\Delta_k^\tau \Delta_k^v) = E(\Delta_k^\tau \Delta_k^\lambda) = 0$. This is due to the fact that the different noise terms show no significant correlation in experiments. After averaging, we have in the first nonvanishing order

$$\overline{v}=\overline{\lambda}[\overline{v}^{1-\alpha}+f_{\alpha}(1-\alpha)\overline{\tau}]^{1/(1-\alpha)} \times\ldots\times\left[1+a_{2}(\overline{v})\mathcal{C}_{v}^{2}+b_{2}(\overline{v})\mathcal{C}_{\tau}^{2}\right]. \tag{B6}$$

We square Eq. (B6) and average over the noise terms up to second order. This time we obtain

$$(1+\mathcal{C}_{v}^{2})=\overline{\lambda}^{2}(1+\mathcal{C}_{\lambda}^{2})\left(1+\frac{f_{\alpha}(1-\alpha)\overline{\tau}}{\overline{v}^{1-\alpha}}\right)^{2/(1-\alpha)} \times\cdots\times\left\{1+[a_{1}^{2}(\overline{v})+2a_{2}(\overline{v})]\mathcal{C}_{v}^{2} +\cdots+\left[b_{1}^{2}(\overline{v})+2b_{2}(\overline{v})\right]\mathcal{C}_{\tau}^{2}\right\}. \tag{B7}$$

Both Eqs. (B6) and (B7) determine the average size $\overline{v}$ and the coefficient of variation $\mathcal{C}_v$ as functions of stochastic fluctuations $\mathcal{C}_\tau$ and $\mathcal{C}_\lambda$, as well as the system parameters α, f_α, $\overline{\tau}$, and $\overline{\lambda}$.

If we assume $\mathcal{C}_\tau \approx 0$, the coefficients a_1 and a_2 can be easily determined. After a short calculation we arrive at the relations

$$\overline{v}=\overline{\lambda}[\overline{v}^{1-\alpha}+f_{\alpha}(1-\alpha)\overline{\tau}]^{1/(1-\alpha)} \times\cdots\times\left(1-\frac{1}{2}\frac{\alpha f_{\alpha}(1-\alpha)\overline{\tau}\,\overline{v}^{1-\alpha}}{[\overline{v}^{1-\alpha}+f_{\alpha}(1-\alpha)\overline{\tau}]^{2}}\mathcal{C}_{v}^{2}\right) \tag{B8}$$

and

$$\overline{v}^{2}=\overline{\lambda}^{2}\frac{1+\mathcal{C}_{\lambda}^{2}}{1+\mathcal{C}_{v}^{2}}[\overline{v}^{1-\alpha}+f_{\alpha}(1-\alpha)\overline{\tau}]^{2/(1-\alpha)} \times\cdots\times\left(1+\frac{\overline{v}^{1-\alpha}(\overline{v}^{1-\alpha}-\alpha(1-\alpha)f_{\alpha}\overline{\tau})}{[\overline{v}^{1-\alpha}+(1-\alpha)f_{\alpha}\overline{\tau}]^{2}}\mathcal{C}_{v}^{2}\right). \tag{B9}$$

By replacing $\mathcal{C}_v$ in Eq. (B8) with Eq. (B9), we obtain an implicit relation for $\overline{v}$. The first-order approximation of the problem neglects the impact of $\mathcal{C}_v$ in (B8) and thus results in Eqs. (B10) and (10). Thus, in lowest order we have the steady-state solution of Eq. (3),

$$\overline{v}=\left(\frac{f_{\alpha}(1-\alpha)\overline{\tau}}{\overline{\lambda}^{1-\alpha}-1}\right)^{1/(1-\alpha)}. \tag{B10}$$

This equation constitutes a decent approximation if $\mathcal{C}_\tau$ and $\mathcal{C}_\lambda$ are sufficiently small.

Equation (B1) allows us to assess the functional form of $\Phi(v)$. By definition, the distribution is centered around the mean value $\overline{v}$. The different contributions of the noise terms broaden the distribution function, where the linearization around the steady state results in $u_{k+1} = \gamma u_k + \xi_k^1 + \xi_k^2$, with $\ln v_k/\overline{v} = u_k$. The expectation values of the random numbers ξ^1 and ξ^2 are 0. Provided the noise terms ξ^1 and ξ^2 are Gaussian, the distribution of u itself exhibits the form of a Gaussian distribution.

Even if the noise deviates from a normal distribution, we will likely see convergence according to the central limit theorem. The question is how fast the prefactor γ in an infinite sum declines. If γ is close to 1, which is the case for small values of $1-\alpha$, the sum $u_k = \xi_k^1 + \gamma\xi_{k-1}^1 + \gamma^2\xi_{k-2}^1 + \cdots$ will eventually converge to a normal distribution. The variation coefficient of u is approximately given by Eq. (10). Accordingly, the standard deviation of the log-normal distribution is determined by

$$\sigma=\sqrt{\ln\left(\mathcal{C}_{v}^{2}+1\right)}. \tag{B11}$$

After rewriting Eq. (B1) as the infinite sum of random numbers with zero mean and decreasing standard deviation, we finally obtain the expression

$$\Phi(v)\sim\frac{1}{v}\exp\left(-\frac{(\ln v-\ln\overline{v}+\ln\sqrt{\mathcal{C}_{v}^{2}+1})^{2}}{2\ln(\mathcal{C}_{v}^{2}+1)}\right),$$

to which both random processes contribute via $\mathcal{C}_v$ and $\overline{v}$. Equation (B12) is utilized for calculations of the conditional size distribution in two consecutive cell cycles. This is central for Sec. IV B. We encounter two conditional size distributions $P(v_k|v_{k+1})$ and $P(v_{k+1}|v_k)$, where the first tells us about the likelihood that cells with size v_{k+1} originate from cells with size v_k. According to the Bayes theorem, we have

$$P(v_{k}|v_{k+1})\sim P(v_{k+1}|v_{k})\Phi(v_{k}), \tag{B12}$$

which is used to calculate the conditional average $\mu_k|v_{k+1}$ of the cell size v_k. In Eq. (B12) the conditional probability $P(v_{k+1}|v_k)$ can be expressed by the help of the hazard function $p(\tau)$ of the cell division process. Since division is assumed to be age controlled, we obtain a survival probability $\Psi^{(S)}(\tau)$ that is linked to the division rate function by the fundamental relation

$$\Psi^{(S)}(\tau)=p(\tau)\exp\left(-\int_{0}^{\tau}dtp(t)\right). \tag{B13}$$

After replacing τ in Eq. (B13) with v_k and $\overline{N}v_{k+1}$ as terms of the growth process (2), we obtain the sought relation for $P(v_{k+1}|v_k) \sim \Psi^{(S)}(\tau)$. Calculations of the conditional mean value and standard deviation can now be performed by evaluating

$$m_{n}|v_{k+1}\sim\int_{0}^{\infty}dx\,x^{n-\alpha}\Psi^{(S)}\left(\frac{\overline{N}^{1-\alpha}v_{k+1}^{1-\alpha}-x^{1-\alpha}}{f_{\alpha}(1-\alpha)}\right)\Phi(x). \tag{B14}$$

For $\alpha \to 1$ we obtain the relations of Sec. IV B.

APPENDIX C: CORRELATION BETWEEN SIZE v AND STARCH CONTENT y

The discrete stochastic process for the deviation from the average cell volume is given by

$$\Delta_{k+1}^{v}=N^{\alpha-1}\Delta_{k}^{v}+\ln N\Delta_{k}^{\tau}+\Delta_{k}^{\lambda} =\sum_{l=0}^{\infty}N^{l(\alpha-1)}\left(\ln N\Delta_{k-l}^{\tau}+\Delta_{k-l}^{\lambda}\right). \tag{C1}$$

The second equation integrates all shock terms Δ^{λ} and Δ^{τ} in order to determine the current value of Δ_k^v. We use the discrete-time equation (7) to evaluate the mean value of y_k:

$$\begin{aligned}\overline{y} &= \frac{1}{M\overline{N}-1}\left(\overline{H\left[\frac{v}{\lambda}\right]}-\overline{H[v]}\right)\\ &\approx \frac{1}{M\overline{N}-1}\left(H[\overline{v}\overline{N}]+\frac{1}{2}H''[\overline{v}\overline{N}]\overline{v}^2\overline{N}^2\mathcal{C}_v^2+\cdots\right)\\ &\quad-\frac{1}{M\overline{N}-1}\left(H[\overline{v}]+\frac{1}{2}H''[\overline{v}]\overline{v}^2\mathcal{C}_v^2+\cdots\right).\end{aligned} \tag{C2}$$

In the lowest approximation we have the average

$$\overline{y} = \frac{1}{M\overline{N}-1}[H(\overline{v}\overline{N})-H(\overline{v})]. \tag{C3}$$

Equation (C3) shows that $\overline{y}$ explicitly depends on M. It can be estimated as follows. We introduce a rate function $d_y(v,y)$ that determines the amount of starch as the solution of a decay process that follows

$$\frac{d}{d\tau}y(\tau) = d_y[v,y(\tau)]. \tag{C4}$$

On average the decrease of starch during the dark period has to be balanced by faster accumulation of starch during the preceding light period. This implies that the relative increase of y exceeds the increase of cell volume v. In other words, the density of starch per cell volume, i.e., the ratio $\varrho = y/v$, increases by the factor M, as depicted in Fig. 5.

The function $d_y(v,y)$ has to be specified on grounds of the underlying degradation mechanism. If degradation is assumed to be size dependent, we can tentatively cast the problem into the rate function $d_y(v,y) = -d_y yv$, with $d_y = \text{const}$. The argument here is that the depletion of recourses is likely to proceed faster in large cells. On average the factor M satisfies the balance condition

$$\frac{1}{M} = \exp(-d_y T_{\text{deg}}\overline{v}), \tag{C5}$$

where T_{deg} is the length of the degradation period. Equation (C5) allows us to reformulate $d_y T_{\text{deg}}$ in terms of $\overline{v}$ and M. The particular form of the assumed degradation type introduces the dependence on the stochastic variable v_{k+1}, namely,

$$m_k(v_{k+1}) = \exp\left(-\ln M\frac{v_{k+1}}{\overline{v}}\right). \tag{C6}$$

Equation (C6) makes clear that we will observe no additional fluctuations if m_k is size independent. In this case m_k would simply add a constant factor in front of Eq. (7). If, however, the degradation of starch is dependent on size, we have in the linear response

$$\Delta_k^m \approx -\ln M\Delta_{k+1}^v. \tag{C7}$$

According to Eq. (17), the magnitude of fluctuations decreases for large values of v_{k+1} and the decay in the dark is faster if M becomes large.

For the linearized equation for the shocks Δy we can use

$$\begin{aligned}\Delta_{k+1}^y &= \Delta_k^m+\Delta_k^{\gamma}+\frac{1}{M\overline{N}}\Delta_k^y\\ &\quad+\cdots+\frac{H'[\overline{N}\overline{v}]\overline{v}}{M\overline{y}}\Delta_{k+1}^v-\frac{H'[\overline{v}]\overline{v}}{\overline{N}M\overline{y}}\Delta_k^v.\end{aligned} \tag{C8}$$

Equation (C8) together with the linearization of Eq. (3) can be used to determine the variance of y and v. After multiplying Eq. (C8) with Δ_{k+1}^v and averaging both sides of the equation, the covariance $\text{Cov}(v,y)$ is obtained. The ratio of the covariance and variation coefficients $\mathcal{C}_v$ and $\mathcal{C}_y$ defines the product-moment correlation coefficient $\text{Corr}(v,y)$ after Pearson:

$$\text{Corr}(v,y) = \frac{\text{Cov}(v,y)}{\mathcal{C}_y\mathcal{C}_v}. \tag{C9}$$

Here $\text{Corr}(v,y)$ serves as an orientation for the strength of the correlation between size and starch content. In the case that m_k depends on size and γ_k allows for asymmetric division, we have

$$\begin{aligned}\text{Cov}(v,y) &= \frac{E\left[\Delta_k^m\Delta_{k+1}^v\right]+E\left[\Delta_k^{\gamma}\Delta_{k+1}^v\right]}{M\overline{N}-\overline{N}^{\alpha-1}}\\ &\quad+\cdots+\frac{\mathcal{C}_v^2}{M\overline{N}}\frac{M\overline{N}-1}{M\overline{N}-\overline{N}^{\alpha-1}}\\ &\quad\times\frac{H'[\overline{N}\overline{v}]\overline{N}\overline{v}-H'[\overline{v}]\overline{N}^{\alpha-1}\overline{v}}{H[\overline{N}\overline{v}]-H[\overline{v}]}.\end{aligned} \tag{C10}$$

Averaging of $\Delta_k^m\Delta_{k+1}^v$ results in

$$E\left[\Delta_k^m\Delta_{k+1}^v\right] = -\ln M\mathcal{C}_v^2. \tag{C11}$$

The repeated bisection that produces 2^n DCs implies that γ_k is a function of $2^n = 1/\lambda_k$. The average of $E[\Delta_k^{\gamma}\Delta_{k+1}^v] = E[\Delta_k^{\gamma}\Delta_k^{\lambda}]$ is thus dependent on the number of daughter cells. We can determine $E[\gamma_k\lambda_k]$ and obtain

$$\begin{aligned}E[\gamma_k\lambda_k] &= \frac{1}{\overline{N}^2}E\left[1+\Delta_k^{\gamma}+\Delta_k^{\lambda}+\Delta_k^{\gamma}\Delta_k^{\lambda}\right]\\ &= \frac{1+E[\Delta_k^{\gamma}\Delta_k^{\lambda}]}{\overline{N}^2}.\end{aligned} \tag{C12}$$

Hence, it is possible to determine $E[\Delta_k^{\gamma}\Delta_k^{\lambda}]$ by evaluating $E[\gamma_k\lambda_k]$. The n-fold iteration leads to

$$\gamma_k = \frac{1}{2}\gamma^{(1)}\frac{1}{2}\gamma^{(2)}\cdots\frac{1}{2}\gamma^{(n)} = \frac{1}{2^n}\prod_{l=1}^{n}\gamma^{(l)}, \tag{C13}$$

with $\overline{\gamma^l} = 1$ and $\mathcal{C} = \text{const}$ in each bisection. We find

$$E[\gamma_k\lambda_k] = \sum_n^{\infty}\left[\frac{\pi_n}{2^{2n}}\prod_{l=1}^{n}\gamma^{(l)}\right]. \tag{C14}$$

The product can be approximated by

$$\prod_{l=1}^{n}\gamma^{(l)} = \prod_{l=1}^{n}1+\Delta^{\gamma^{(l)}} \approx 1+\sum_{l=1}^{n}\Delta^{\gamma^{(l)}}. \tag{C15}$$

It is further assumed that the random terms $\gamma^{(l)}$ describe independent events. Consequently, averaging yields

$E[\gamma_k\lambda_k] = \sum_n^\infty \frac{\pi_n}{2^{2n}}$ and finally

$$E\left[\Delta_k^\gamma \Delta_k^\lambda\right] = \mathcal{C}_\lambda^2. \tag{C16}$$

Similarly, we find for $\mathcal{C}_\gamma$

$$E[\gamma_k\gamma_k] = \frac{1+\mathcal{C}_\gamma^2}{\overline{N}^2} \tag{C17}$$

and

$$E[\gamma_k\gamma_k] = \sum_n^\infty \left[\frac{\pi_n}{2^{2n}} \prod_{l=1}^n (1+\Delta^{\gamma^{(l)}})^2\right] = \sum_n^\infty \left[\frac{\pi_n}{2^{2n}}(1+\mathcal{C}^2)^n\right]. \tag{C18}$$

The variation coefficient for y is obtained after squaring and averaging Eq. (C8). After the adiabatic elimination of Δ_k^y for $\overline{N} \gg 1$ calculations further simplify. For $\mathcal{C}_\lambda = 0$ and $\alpha = 1$ we find the covariance

$$\mathrm{Cov}(v,y) \approx \frac{\mathcal{C}_v^2}{M\overline{N}}\left(-\frac{\ln M M\overline{N}}{M\overline{N}-1} + \frac{H'[\overline{N}\overline{v}]\overline{N}\overline{v} - H'[\overline{v}]\overline{v}}{H[\overline{N}\overline{v}] - H[\overline{v}]}\right) \tag{C19}$$

and the variation coefficient

$$\mathcal{C}_y^2 \approx \mathcal{C}_v^2\left(\ln M + \frac{H'[\overline{N}\overline{v}]\overline{N}\overline{v} - H'[\overline{v}]\overline{v}}{H[\overline{N}\overline{v}] - H[\overline{v}]}\right)^2. \tag{C20}$$

Equation (C19) shows that $\mathrm{Cov}(v,y)$ and therefore $\mathrm{Corr}(v,y)$ are decreasing functions in M, which can vanish for certain values of the parameters $\overline{N}$, $\overline{v}$, and M (see Fig. 6). According to Eq. (C19), there is a simple zero that defines the value M' for which the product-moment correlation vanishes. For example, the case $H \approx cv$ gives $M' \approx 2.71$, while a concave function $h(v)$ entails a smaller value of M'.

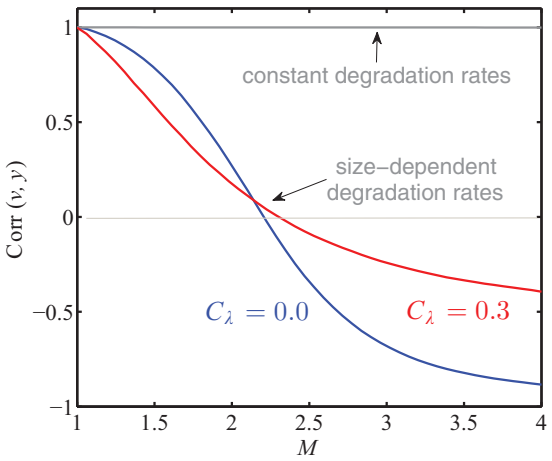

FIG. 6. (Color online) Correlation coefficient as a function of M. The parameter M describes the difference of the growth process between y and v. In the case of constant degradation the correlation between the parameters is always close to 1, while size-dependent degradation of starch decreases the correlation between both parameters. The plot shows that the decrease of the correlation depends also on the strength of the coefficient of variation (indicated here with $\mathcal{C}$): For $\mathcal{C}_\lambda = 0$ the decrease of the correlation is slow at small M and and it is stark at intermediate values of M; for $\mathcal{C}_\lambda = 0.3$ the decrease of the correlations is fast at small M and slow at large values of M.

[1] D. Drake and K. Brogden, *Polymicrobial Diseases* (ASM, Washington, DC, 2002).
[2] D. J. Ferullo, D. L. Cooper, H. R. Moore, and S. T. Lovett, Methods **48**, 8 (2009).
[3] E. Bernstein, Science **131**, 1528 (1960).
[4] T. Cools, A. Iantcheva, S. Maes, H. Van Den Daele, and L. De Veylder, Plant J. **64**, 705 (2010).
[5] G. Balázsi, A. Van Oudenaarden, and J. J. Collins, Cell **144**, 910 (2011).
[6] M. Sturrock, A. Hellander, A. Matzavinos, and M. A. J. Chaplain, J. R. Soc. Interface **10**, 20120988 (2013).
[7] M. Thattai and A. Van Oudenaarden, Proc. Natl. Acad. Sci. USA **98**, 8614 (2001).
[8] B. Alberts, D. Bray, J. Lewis, M. Raff, K. Roberts, and J. D. Watson, *Molecular Biology of the Cell*, 3rd ed. (Garland Science, New York, 2010).
[9] L. Donnan, E. P. Carvill, T. J. Gilliland, and P. C. L. John, New Phytol. **99**, 1 (1985).
[10] K. Bišová and V. Zachleder, J. Exp. Bot. **65**, 2585 (2014).
[11] A. Garz, M. Sandmann, M. Rading, S. Ramm, R. Menzel, and M. Steup, Biophys. J. **103**, 1078 (2012).
[12] M. McAteer, L. Donnan, and P. C. L. John, New Phytol. **99**, 41 (1985).
[13] H. Oldenhof, V. Zachleder, and H. van den Ende, Folia Microbiol. **53**, 52 (2007).
[14] P. Fantes and P. Nurse, in *The Cell Cycle*, edited by P. C. L. John (Cambridge University Press, Cambridge, 1981), p. 11.
[15] M. M. Rading, T. A. Engel, R. Lipowsky, and A. Valleriani, J. Stat. Phys. **145**, 1 (2011).
[16] K. Matsumura, T. Yagi, and K. Yasuda, Biochem. Biophys. Res. Commun. **306**, 1042 (2003).
[17] G. Webb, Math. Biosci. **85**, 71 (1987).
[18] N. Brenner, K. Farkash, and E. Braun, Phys. Biol. **3**, 172 (2006).
[19] N. Brenner and Y. Shokef, Phys. Rev. Lett. **99**, 138102 (2007).
[20] D. Ramkrishna, Math. Biosci. **12**, 123 (1969).
[21] J. L. Spudich and R. Sager, J. Cell Biol. **85**, 136 (1980).
[22] M. Kazunori, Y. Toshiki, H. Akihiro, S. Mikhail, and Y. Kenji, J. Nanobiotechnol. **8**, 23 (2010).
[23] T. Kuczek, Math. Biosci. **69**, 159 (1984).
[24] B. H. Shah, J. D. Borwanker, and D. Ramkrishna, Math. Biosci. **31**, 1 (1976).
[25] E. H. Harris, Annu. Rev. Plant Physiol. Plant Mol. Biol. **52**, 363 (2001).